

Cytotoxic Isomalabaricane Derivatives and a Monocyclic Triterpene Glycoside from the Sponge *Rhabdastrella globostellata*

Miyabi Hirashima,[†] Kazuomi Tsuda,[†] Toshiyuki Hamada,[†] Hiroaki Okamura,[†] Tatsuhiko Furukawa,[‡] Shin-ichi Akiyama,[‡] Yusuke Tajitsu,[§] Ryuji Ikeda,[§] Masaharu Komatsu,[⊥] Matsumi Doe,^{||} Yoshiki Morimoto,^{||} Motoo Shiro,[∇] Rob W. M. van Soest,[△] Kaoru Takemura,[¶] and Tetsuo Iwagawa^{*†}

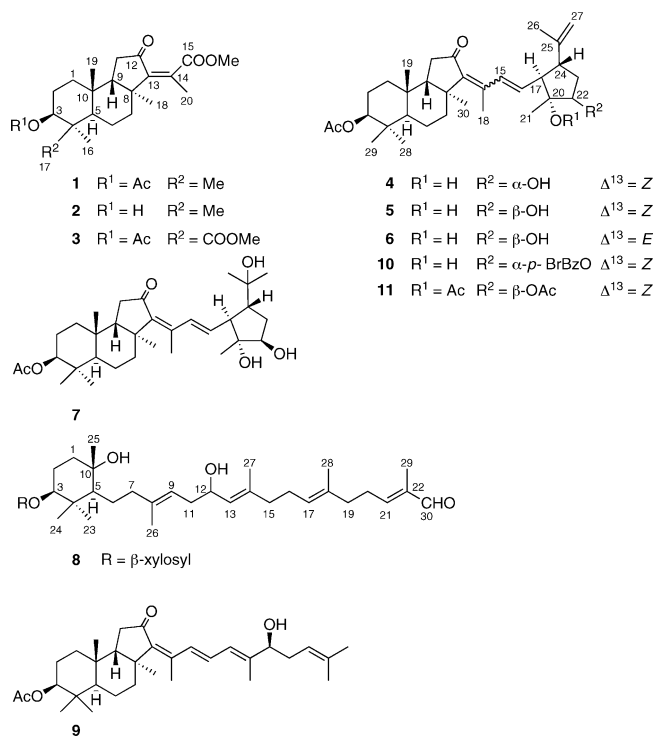
Department of Chemistry and Bioscience, Graduate School of Science and Engineering, Kagoshima University, 1-21-35 Korimoto, Kagoshima 890-0065, Japan, Department of Molecular Oncology and Department of Clinical Pharmacy and Pharmacology, Graduate School of Medical and Dental Sciences, Kagoshima University, 8-35-1 Sakuragaoka, Kagoshima, 890-8520, Japan, Department of Food and Chemical Biology, Faculty of Fisheries, Kagoshima University, 4-5-20 Shimoarata, Kagoshima 890-0065, Japan, Department of Chemistry, Graduate School of Science, Osaka City University, 3-3-138 Sugimoto, Sumiyoshi-ku, Osaka 558-8585, Japan, Rigaku Corporation 3-9-12 Matsubaracho Akishima-shi, Tokyo 196-8666, Japan, Department of Coelenterates and Porifera (Zoologisch Museum), University of Amsterdam, P.O. Box 94766, 1090 GT Amsterdam, The Netherlands, and Sankei Chemical Co., Ltd. 2-9 Nan'ei-chou, Kagoshima 891-0122, Japan

Received May 5, 2010

Seven new isomalabaricane derivatives, rhabdastins A–G (**1–7**), and a new monocyclic triterpene glycoside, rhabdastoside A (**8**), have been isolated from the methanol extract of the sponge *Rhabdastrella globostellata*, collected at Amami-oshima, Japan. Three of them were isolated as their corresponding methyl esters, rhabdastins A–D (**1–3**). Their structures were determined on the basis of spectroscopic and X-ray diffraction analyses. The isolated compounds were evaluated for their cytotoxicity against the proliferation of promyelocytic leukemia HL-60 cells. Compounds **4**, **5**, **7**, and **11**, possessing a cyclopentane side chain, exhibited weak activity, with IC₅₀ values of 21, 29, 44, and 11 μM, respectively, while compounds **1**, **2**, and **3**, with a 2-substituted-propanoate side chain, were inactive at 100 μM. In addition, the mechanism of cytotoxicity of compounds **4** and **5** was investigated.

Although the orange to brown colored sponges belonging to the genus *Rhabdastrella* are conspicuous and soft, they do not appear to be preyed upon by other animals. This may be due to the presence of bioactive defensive metabolites within the sponges. Because it is often argued that naturally occurring biologically active compounds may have additional activities, such as the ability to kill human pathogens and cancer cells, compounds from sponges of this genus may be worthy of investigation for new lead compounds.¹ Sponges of the genus *Rhabdastrella* have been investigated extensively and have been reported to produce a range of isomalabaricane triterpenes possessing a tricyclic nucleus with *trans*–*syn*–*trans* ring junctions.² The majority of them also have exhibited interesting biological activities, such as cytotoxicity against HL-60, HUVE, and L5178Y cells³ and promotion of DNA binding to DNA polymerase β.⁴

In a continuation of our survey of bioactive compounds from marine organisms,^{5–9} the CH₂Cl₂-soluble portion of a MeOH extract of the marine sponge *Rhabdastrella globostellata*, collected at Amami-oshima, Japan, showed strong cytotoxic activity (IC₅₀ = 4.6 μg/mL) against proliferation of human promyelocytic leukemia cells (HL-60). Further investigation of this CH₂Cl₂ portion has led to the isolation of seven new isomalabaricanes, rhabdastins A–C (**1–3**) as methyl esters and rhabdastins D–G (**4–7**), and a monocyclic triterpene glycoside, rhabdastoside A (**8**). In this paper, we describe the structure elucidation of these compounds and propose a mechanism of cytotoxicity of **4** and **5** against HL-60.



* To whom correspondence should be addressed. Tel: +81-99-285-8115. Fax: +81-99-285-8117. E-mail: iwagawa@sci.kagoshima-u.ac.jp.

[†] Department of Chemistry and Bioscience, Kagoshima University.

[‡] Department of Molecular Oncology, Kagoshima University.

[§] Department of Clinical Pharmacy and Pharmacology, Kagoshima University.

[⊥] Department of Food and Chemical Biology, Kagoshima University.

^{||} Osaka City University.

[∇] Rigaku Corporation.

[△] University of Amsterdam.

[¶] Sankei Chemical Co., Ltd.

Results and Discussion

A MeOH extract of the sponge (1.2 kg, dry wt) was suspended in H₂O and then extracted with CH₂Cl₂ to give an organic extract (28.1 g) that showed cytotoxic activity against HL-60 cells. A portion of the CH₂Cl₂ extract (7.1 g) was subjected to silica gel column chromatography and elution with mixtures of CH₂Cl₂/MeOH with increasing polarity to afford a fraction, which was further investigated. The ¹H NMR spectrum of the fraction indicated the absence of carbomethoxy signals. The fraction was then esterified with trimethylsilyldiazomethane, as it included an acidic material that prevented further separation due to tailing. The

Table 1. ^{13}C NMR Spectroscopic Data (150 MHz, CDCl_3) for Rhabdastins A–G (1–7)

position	1		2		3		4		5		6		7	
1	33.1,	CH_2	33.4,	CH_2	29.4,	CH_2	33.1,	CH_2	32.9,	CH_2	32.9,	CH_2	33	CH_2
2	25.0,	CH_2	28.9,	CH_2	24.9,	CH_2	25.1,	CH_2	25.0,	CH_2	25.0,	CH_2	25.1,	CH_2
3	80.6,	CH	79.2,	CH	73.5,	CH	80.8	CH	80.8,	CH	80.8,	CH	80.8,	CH
4	38.2,	C	39.1,	C	47.1,	C	38.2	C	38.1,	C	38.0,	C	38.2,	C
5	46.6,	CH	46.5,	CH	41.9,	CH	46.6	CH	46.5,	CH	46.6,	CH	46.6,	CH
6	17.8,	CH_2	17.9,	CH_2	19.6,	CH_2	18.2	CH_2	18.1,	CH_2	18.3,	CH_2	18.2,	CH_2
7	36.2,	CH_2	36.3,	CH_2	36.6,	CH_2	38.1	CH_2	38.1,	CH_2	39.0,	CH_2	38.2,	CH_2
8	42.8,	C	42.9,	C	42.9,	C	44.3	C	44.2,	C	44.2,	C	44.3,	C
9	50.6,	CH	50.7,	CH	49.9,	CH	50.3	CH	50.1,	CH	50.1,	CH	50.3,	CH
10	35.5,	C	35.6,	C	35.7,	C	35.4	C	35.3,	C	35.3,	C	35.4,	C
11	34.6,	CH_2	34.6,	CH_2	34.6,	CH_2	36.6	CH_2	36.7,	CH_2	36.5,	CH_2	36.7,	CH_2
12	203.6,	C	203.8,	C	203.6,	C	206.7	C	206.9,	C	208.2,	C	206.8,	C
13	146.8,	C	146.9,	C	146.6,	C	145.4	C	146.3,	C	146.0,	C	145.4,	C
14	133.9,	C	133.8,	C	134.1,	C	141.9	C	141.9,	C	140.8,	C	142.0,	C
15	171.8,	C	171.8,	C	171.8,	C	132.9	CH	132.7,	CH	133.2,	CH	131.4,	CH
16	29.0,	CH_3	29.0,	CH_3	23.1,	CH_3	134.3	CH	134.5,	CH	136.3,	CH	136.8,	CH
17	16.9,	CH_3	15.9,	CH_3	176.5,	CH_3	53.7	CH	54.7,	CH	55.3,	CH	52.0,	CH
18	24.6,	CH_3	24.7,	CH_3	24.4,	CH_3	16.4	CH_3	16.3,	CH_3	14.7,	CH_3	16.4,	CH_3
19	22.4,	CH_3	22.3,	CH_3	19.6,	CH_3	22.4	CH_3	22.2,	CH_3	22.0,	CH_3	22.3,	CH_3
20	16.6,	CH_3	16.6,	CH_3	16.6,	CH_3	81.1	C	82.1,	C	82.1,	C	81.6,	C
21							21.4	CH_3	16.8 ^a ,	CH_3	17.1,	CH_3	21.1,	CH_3
22							77.4	CH	79.1,	CH	79.2,	CH	77.8,	CH
23							36.1	CH_2	34.2,	CH_2	34.3,	CH_2	31.9,	CH_2
24							47.4	CH	45.9,	CH	46.1,	CH	49.8,	CH
25							146.1	C	145.6,	C	146.0,	C	72.5,	C
26							19.4	CH_3	19.7,	CH_3	19.7,	CH_3	29.0,	CH_3
27							111.0	CH_2	110.9,	CH_2	110.0,	CH_2	29.1,	CH_3
28							29.0	CH_3	28.9,	CH_3	28.9,	CH_3	29.0,	CH_3
29							16.9	CH_3	16.7 ^a ,	CH_3	16.8,	CH_3	16.9,	CH_3
30							24.7	CH_3	24.6,	CH_3	25.4,	CH_3	24.8,	CH_3
MeCO	21.2,	CH_3			21.2	CH_3	21.2	CH_3	21.1,	CH_3	21.1,	CH_3	21.2,	CH_3
MeCO	171.0,	C			169.9	C	171.0	C	171.3,	C	171.3,	C	171.0,	C
4-COOMe					51.5	CH_3								
14-COOMe	52.4,	CH_3	52.4,	CH_3	52.4	CH_3								

^a These values may be interchanged.

resulting esterified material was repeatedly subjected to silica gel column chromatography with mixtures of $\text{MeOH}/\text{CH}_2\text{Cl}_2$. Final purification was performed by HPLC on a C_{18} column eluting with mixtures of $\text{MeOH}/\text{H}_2\text{O}$ and/or $\text{MeCN}/\text{H}_2\text{O}$ to give rhabdastins A–G (1–7) and rhabdastoside A (8), which are isomalabaricanes and a monocyclic triterpene glycoside derivative, respectively.

Rhabdastin A (1) was isolated as an amorphous powder, and the molecular formula was determined to be $\text{C}_{23}\text{H}_{34}\text{O}_5$ (seven double-bond equivalents) on the basis of HRFABMS. The IR spectrum indicated absorptions due to an ester carbonyl group at ν_{max} 1732 cm^{-1} , a carbonyl at 1723 cm^{-1} , and an olefin at 1640 cm^{-1} . The ^{13}C NMR spectrum exhibited resonances that were ascribed to two quaternary olefinic carbons at δ 133.9, 146.8 (C-14, C-13), acetyl carbons at δ 21.2, 171.0, an ester carbonyl at δ 171.8 (C-15), and a ketone at δ 203.6 (C-12) (Table 1), accounting for four degrees of unsaturation and indicating that the compound has a tricyclic structure. The ^1H NMR spectrum was similar to those of stelliferin A (9) isolated from the same genus,¹⁰ except for differences in the resonances associated with the side chain at C-13 (Table 1). Thus, resonances due to four methyl singlets at δ 0.89, 0.92, 1.02, 1.35 (Me-17, Me-16, Me-19, Me-18, respectively), an olefinic methyl group at δ 1.98 (Me-20), and a carbomethoxy group (δ 3.80) were observed (Table 2). The configuration of the rings and the asymmetric centers were assigned on the basis of the analysis of the NMR spectra. Thus, the H-3 proton (δ 4.55, dd, $J = 11.7, 5.1\text{ Hz}$) attached to a carbon bearing an acetoxy group (δ 2.06, 3H, s) was identified as axial on the basis of the coupling constant ($J = 11.7\text{ Hz}$). Furthermore it could be shown that H-5, Me-16, and Me-18 were all on the same face (α) of the ring system as H-3, on the basis of the NOESY correlations from H-5 (δ 1.77, $J = 12.3\text{ Hz}$, axial) to H-3, Me-16 (δ 0.92) and Me-18 (δ 1.35). Additional NOESY correlations between Me-19 (δ 1.02) and H-9 (δ 1.88, dd, $J = 13.2, 9.3\text{ Hz}$) and Me-17 (δ 0.89) indicated that these protons were situated on the opposite face (β) to H-3.¹⁰ The

vinyl methyl Me-20 (δ 1.98) and carbomethoxy group (δ 3.80) were attached to C-14 (δ 133.9), on the basis of their correlation to C-14 in the HMBC spectrum. The 13Z geometry was deduced from the NOE correlations between Me-18 and Me-20, leading to the proposed structure 1 for rhabdastin A as the methyl ester derivative.

The ^1H NMR spectra of the methyl ester derivatives, rhabdastin B (2), $\text{C}_{21}\text{H}_{32}\text{O}_4$, and rhabdastin C (3), $\text{C}_{24}\text{H}_{34}\text{O}_7$, were similar to that of 1, except for the absence of an acetyl group in 2 and the presence of two carbomethoxy groups in 3. This was readily detected in the ^1H NMR spectrum of 2, which showed that the signal for H-3 (δ 3.30, 1H, dd, $J = 11.6$ and 5.0 Hz) was shifted upfield by 1.25 ppm when compared with that of 1. Therefore, compound 2 was concluded to be the 3-O-deacetyl derivative of rhabdastin A. The location of the additional carbomethoxy group in compound 3 was identified as C-4, on the basis of the HMBC correlations from the carbomethoxy protons (δ 3.66) to C-3 (δ 73.5), C-4 (δ 47.1), and the ester carbonyl (δ 176.5). The β -orientation of the group was established from an NOE observation between the carbomethoxy protons and Me-19 (δ 0.82). Thus, the structure of rhabdastin C is shown as 3.

Rhabdastin D (4) was isolated as a pale yellow, amorphous powder with the molecular formula $\text{C}_{32}\text{H}_{48}\text{O}_5$. The IR spectrum indicated the presence of a hydroxy group (ν_{max} 3430 cm^{-1}), an ester (ν_{max} 1732 cm^{-1}), a conjugated carbonyl (ν_{max} 1694 cm^{-1}), and a conjugated olefinic group (ν_{max} 1622 cm^{-1}). The ^{13}C NMR spectrum identified resonances assigned to six olefinic carbons at δ 111.0, 132.9, 134.3, 141.9, 145.4, 146.1 (C-27, C-15, C-16, C-14, C-13, C-25, respectively), an acetyl group (δ 21.2, 171.0), and a ketone at δ 206.7, suggesting that the compound has a tetracyclic structure. In the ^1H NMR spectrum, resonances due to the A–C rings were similar to those of 1 and accounted for three rings. Thus it was postulated that the fourth ring was located in the side chain beginning at C-14, which now displayed a more complex pattern

Table 2. ¹H NMR Spectroscopic Data (600 MHz, CDCl₃) for Rhabdastins A–G (1–7)

position	1	2	3	4	5	6	7
1α	1.59, ddd (12.9, 12.9, 3.9)	1.53, ddd (12.8, 12.8, 3.8)	1.72, ddd (13.4, 13.4, 4.4)	1.60 ^a	1.60 ^a	1.59, ddd (12.8, 12.8, 3.6)	1.60, ddd (13.1, 13.1, 3.3)
1β	1.40, ddd (12.9, 3.9, 3.4)	1.40, m	1.20 ^a	1.39, ddd (9.6, 3.3, 3.3)	1.38, ddd (9.6, 3.3, 3.3)	1.39, ddd (12.8, 3.6, 3.6)	1.39, m
2α	1.84, m	1.82, m	1.78, m	1.84 ^a	1.82 ^a	1.82, m	1.83, m
2β	1.72, m	1.67 ^a	2.17 ^a	1.71 ^a	1.71 ^a	1.69, m	1.70, m
3	4.55, dd (11.7, 5.1)	3.30, dd (11.6, 5.0)	5.43, m	4.55, dd (11.7, 5.1)	4.55, dd (11.7, 5.1)	4.56, dd (11.7, 5.1)	4.55, dd (11.6, 5.1)
5	1.77, br d (12.3)	1.69 ^a	2.41, br d (11.8)	1.76, d (12.3)	1.76, d (12.3)	1.76 ^a	1.76, br d (14.7)
6α	1.72 ^a	1.74, m	1.93 ^a	1.68, m	1.69, m	1.67 ^a	1.68, m
6β	1.49, m	1.48, m	1.82, m	1.47, m	1.46, m	1.46, m	1.47, m
7α	2.00, m	2.00, m	2.04, m	2.04, m	2.04, m	2.02 ^a	2.01–2.14, m
7β	2.16 ^a	2.16, m	2.20, m	2.12, m	2.12, m	2.12, m	
8							
9	1.88, dd (13.2, 9.3)	1.88, dd (13.4, 9.3)	1.93 ^a	1.81 ^a	1.79 ^a	1.78, m	1.82, m
11α	2.17 ^a	2.18 ^a	2.18, m	2.16, m	2.15–2.26, m	2.18, m	2.11–2.24, m
11β		2.18 ^a	1.84, m	2.19, m		2.18, m	
15				7.74, d (15.9)	7.81, d (15.9)	6.43, d (15.6)	7.79, d (15.9)
16	0.92, br s	1.03, br s	1.19, br s	5.92, dd (15.9, 8.7)	5.92, dd (15.9, 7.8)	6.02, dd (15.6, 7.7)	6.02, dd (15.9, 8.3)
17	0.89, br s	0.83, br s		2.77, dd (10.6, 8.7)	2.56 ^a	2.58 ^a	2.79, d (8.3)
18	1.35, s	1.34, s	1.38, br s	1.96, s	1.96, s	2.26, br s	1.96, s
19	1.02, br s	1.00, br s	0.82, br s	1.01, br s	1.01, br s	1.01, br s	1.01, br s
20	1.98, s	1.98, s	2.00, s				
21							
22				1.09, s	1.10, br s	1.16, br s	1.06, s
23α				3.74, dd (5.7, 2.1)	4.07, t (8.7)	4.08, t (8.4)	3.67, m
23β				1.62 ^a	2.01, m	2.02 ^a	1.75, m
24				2.21, m	1.74 ^a	1.74 ^a	2.09, m
26				2.46, m	2.59 ^a	2.58 ^a	1.96 ^a
27				1.71, br s	1.72, br s	1.72, br s	1.22, br s
28				4.71, 4.76, br s	4.71, 4.75, br s	4.72, 4.73, br s	1.23, br s
29				0.91, br s	0.91, br s	0.92, br s	0.91, br s
30				0.89, s	0.88, s	0.89, br s	0.89, s
MeCO	2.06, s		2.09, s	1.35, s	1.36, s	1.35, br s	1.36, s
4-COOMe			3.81, s	2.06, s	2.06, s	2.06, s	2.06, s
14-COOMe	3.80, s	3.80, s	3.66, s				

^a Overlapping signals. ^b These values may be interchanged.

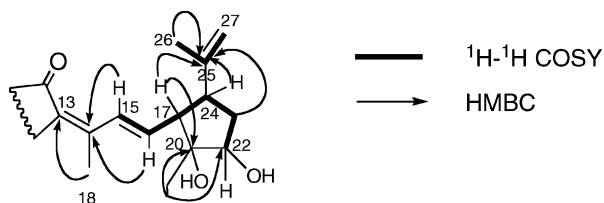


Figure 1. Selected ^1H - ^1H COSY and HMBC correlations of **4**.

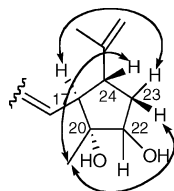


Figure 2. Selected NOESY correlations of **4**.

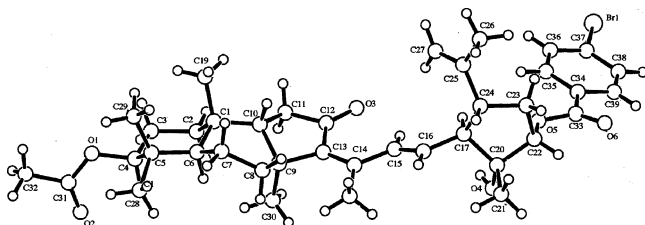


Figure 3. X-ray diffraction structure of **10**.

of resonances than compounds **1**–**3**. These new resonances were assigned to two olefinic methyls, Me-26 (δ 1.71) and Me-18 (δ 1.96), a singlet methyl group at δ 1.09 (Me-21), a methylene at δ 1.62, 2.21 (H₂-23), three methines at δ 2.46 (H-24), 2.77 (H-17), 3.74 (H-22), a terminal vinyl group at δ 4.71, 4.76, (H₂-27), and two olefinic protons at δ 5.92 (H-16) and 7.74, (H-15). Analysis of the ^1H - ^1H COSY spectrum of **4** (Figure 1) indicated the connectivities from H-15 to H-17 and from H-17 to H-22 through H-24 and H₂-23, and Me-26 to H-27. The tertiary carbon C-20 bearing oxygen (δ 81.1) and Me-21 were placed between C-17 (δ 53.7) and C-22 (δ 77.4), on the basis of HMBC correlations from Me-21 to C-20 and C-22 and from H-17 to C-20 (Figure 1). These data established the fourth ring as a substituted cyclopentane. Further HMBC correlations were observed between C-25 (δ 146.1, s) and H-17, H₂-23, H-24, and Me-26, suggesting that C-24 (δ 145.4) and C-25 were contiguous. Connectivities between C-13 (δ 145.4) and C-14 (δ 141.9) and between C-14 and C-15 were supported by the observation of HMBC correlations of Me-18 to C-13 and of H-15 and H-16 to C-14, respectively. On the above data, the gross structure of **4** was deduced, as depicted in Figure 1. The geometries of Δ^{13} and Δ^{15} were elucidated to be *Z* and *E* by the low-field chemical shift of H-15 (δ 7.74)¹⁰ and the large $^3J_{\text{HH}}$ coupling ($J = 15.9$ Hz) between H-15 and H-16. The relative configuration of the cyclopentane ring substituents was inferred by interpretation of the NOESY spectrum (Figure 2). NOE correlations from Me-21 to H-23 (δ 2.21) and H-24 indicated that these protons were situated on the same face (β). H-17 showed a correlation with H-23 (δ 1.62), suggesting an α -orientation for these protons. The relative configuration of the hydroxy group at C-22 could not be determined, because a correlation between H-22 and H-17 or H-24 was not observed. To establish the absolute configuration of **4**, an X-ray diffraction experiment of the 22-*O*-*p*-bromobenzoyl derivative (**10**) was undertaken. The absolute configuration of **10** was determined on the basis of the Flack parameter, $-0.023(9)$, using 2829 Friedel pairs¹¹ (Supporting Information). From the computer-generated perspective drawing of the final X-ray model (Figure 3), the configurations of the nine asymmetric centers in rhabdastin D were assigned as 3*S*, 5*R*, 8*S*, 9*S*, 10*R*, 17*S*, 20*R*, 22*S*, and 24*R*.

This is the first isolation of an isomalabaricane possessing a cyclopentane ring.

Rhabdastin E (**5**), C₃₂H₄₈O₅, was isomeric with **4**. The ^1H and ^{13}C NMR spectra of **5** were essentially identical to those of **4**, with the only major differences in the cyclopentane ring system. Thus, the chemical shifts of H-22 (δ 4.07, $J = 8.7$ Hz) in the ^1H NMR spectrum and of C-21 (δ 16.8 or 16.7) in the ^{13}C NMR spectrum were shifted downfield by 0.33 ppm and upfield by 4.6 ppm, respectively, when compared with those of **4**. This suggested that **4** and **5** differ in the configuration of the hydroxy groups at C-20 and/or C-22. However, the relative configuration of these ring substituents could not be confirmed by NOESY experiments due to signal overlap of the diagnostic peaks. Fortunately, the diacetate (**11**), prepared by acetylation of **5**, showed NOE correlations from H-17 (δ 3.13, dd, $J = 10.1, 8.4$ Hz) to H-22 (δ 5.53, $J = 7.7, 3.5$ Hz) and from Me-21 (δ 1.34) to H-24 (δ 2.69, $J = 10.2$ Hz). Therefore, H-17 and H-22 were determined to have an α -orientation, while Me-21 and H-24 had a β -orientation.

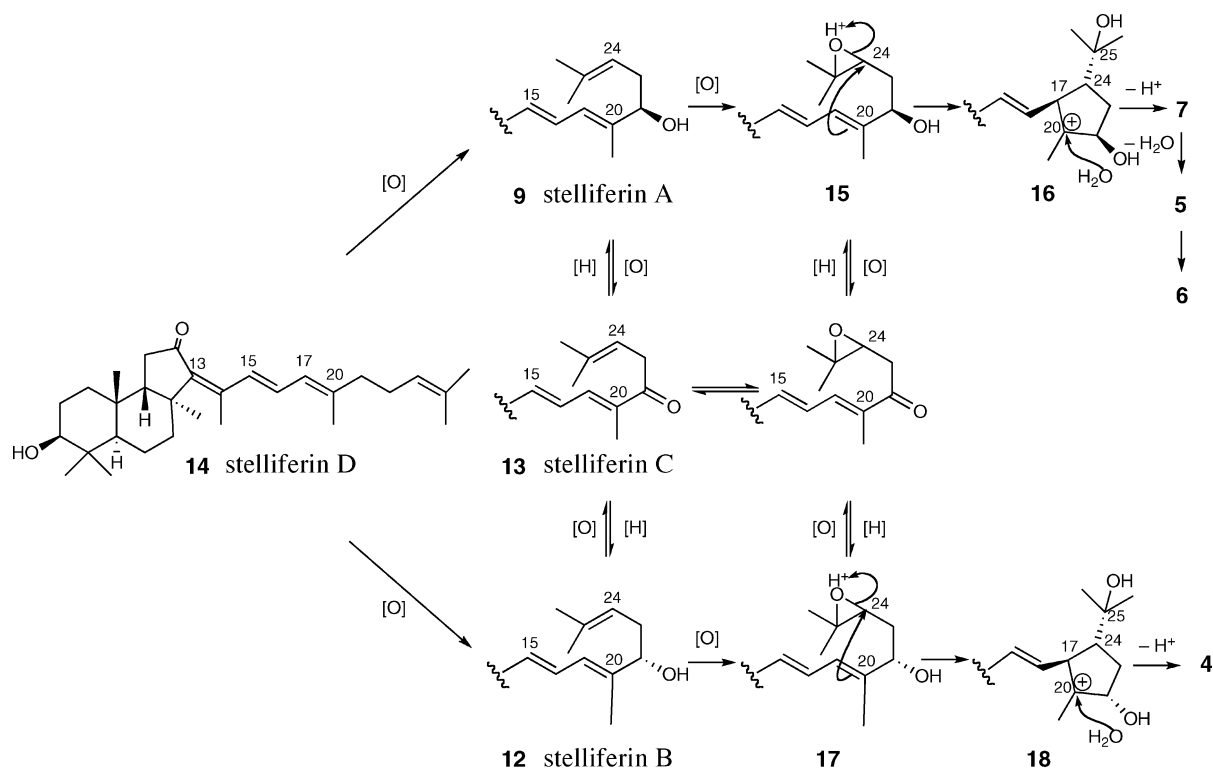
The ^1H NMR spectrum of rhabdastin F (**6**), C₃₂H₄₈O₅, was very similar to that of **5**, except that the chemical shifts of H-15 (δ 6.43) and Me-18 (δ 2.26) were shifted upfield by 1.38 ppm and downfield by 0.3 ppm, respectively, when compared with those of **5**. This indicated that Me-18 was shielded by being closest to the carbonyl group at C-12, while H-15 was deshielded, and hence the geometry of the Δ^{13} double bond was deduced to be *E*.

The molecular formula of rhabdastin G (**7**), C₃₂H₅₀O₆, indicated that the MW of **7** was 18 mass units higher than **5** and **6**. The ^1H and ^{13}C NMR spectra were similar to those of **5**, except that an isopropylene group in **5** was replaced by a 2-hydroxyisopropyl group in **7**. This was further confirmed by the HMBC data, which revealed that the two methyl groups resonating at δ 1.22, 1.23 (C-26, C-27) were correlated to the hydroxyl-bearing carbon C-25 (δ 72.5) and to C-24 (δ 49.8). The relative configuration was determined by the similarity of the NOESY data with those of **5** and **11**.

Compounds **1**–**3** may be formed biogenetically through oxidative cleavage of stelliferin-type compounds. A plausible biogenetic pathway of rhabdastins D–G (**4**–**7**) based on the oxidation and cyclization of various stelliferins is suggested in Scheme 1. For example, epoxidation of the Δ^{24} double bond in stelliferin A (**9**), derived from stelliferin D (**14**),¹⁰ could afford epoxide **15**, which following π -attack by the $\Delta^{17(20)}$ double bond would open the epoxide and yield a tertiary carbocation at C-20 (**16**). Attack by H₂O from the α -face would quench the carbocation to give rhabdastin G (**7**), and dehydration of the hydroxy group at C-25 in **7** would give rhabdastin E (**5**). Rhabdastin F (**6**) may be a photoisomer of **5**, because **5** was gradually converted into **6** under room light. Formation of rhabdastin D (**4**) could arise by a similar pathway from stelliferin B (**12**)¹⁰ via epoxidation to afford **17** followed by epoxide opening to yield the carbocation **18**. Subsequent attack by H₂O on the carbocation from the α -face would give rhabdastin D (**4**). However, as depicted in Scheme 1, alternative biogenetic pathways for compounds **4**–**7** via stelliferin C (**13**)¹⁰ are also possible.

Rhabdastoside A (**8**), C₃₅H₅₈O₈, showed IR absorptions due to a hydroxy group (ν_{max} 3407 cm⁻¹) and an unsaturated carbonyl group (ν_{max} 1672, 1638 cm⁻¹). The molecular formula indicated seven degrees of unsaturation. Eight olefinic carbons resonating at δ 121.0, 125.2, 127.7, 133.7, 138.0, 139.0, 139.4, 154.5 (C-8, C-17, C-13, C-18, C-14, C-8, C-22, C-21, respectively) and a conjugated aldehyde at δ 195.5 (C-30) revealed in the ^{13}C NMR spectrum accounted for five degrees of unsaturation, indicating that the compound contained two rings. The COSY spectrum identified partial structures, **a**, **b**, **c**, **d**, **e**, and **f** (Figure 4) as follows: **a** [H-1' to H₂-5'], **b** [H₂-1 to H-3], **c** [H-5 to H₂-7], **d** [H-9 to H₂-13, H-9 to Me-26, H-13 to Me-27], **e** [H₂-15 through H-17, H-17 to Me-28], and **f** [H₂-19 through H-21, H-21 to Me-29]. The presence of

Scheme 1. Plausible Biogenetic Pathway to 4–7



a β -xylopyranose in **a** was assigned by analysis of five carbon signals from δ 104.5 to 63.8¹⁰ in the ¹³C NMR spectrum and NOESY correlations H-1' (δ 4.50, d, $J = 5.4$ Hz)/H-3' (δ 3.62)/H-5' (δ 3.39) and H-2' (δ 3.50)/H-4' (δ 3.75), as depicted in Figure 5, although the coupling constant of the anomeric proton in the ¹H NMR spectrum was smaller than those reported previously ($J = 6.7$ – 8.9 Hz).¹² The gross structure of **8** was completed by the interpretation of the HMBC experiments, which showed a correlation between H-3 (δ 3.25) and C-4 (δ 40.7), which in turn showed correlations with H-5 (δ 1.17) and the two methyl groups Me-23 (δ 1.04) and Me-24 (δ 0.83). This linked spin system **b** with **c** through C-4. Additional correlations of H₂-1 (δ 1.41, 1.73), H-5, and Me-25 (δ 1.13) with C-10 (δ 72.6) also linked **b** with **c** through C-10 and indicated the presence of a cyclohexane in **8** as the second ring. That the β -xylose was attached at C-3 through a glycosidic linkage was evident from the HMBC correlation from H-3 to C-1' (δ 104.5). Finally, the linkage of spin systems **c**, **d**, **e**, and **f** of the aliphatic side chain was established by a series of HMBC correlations as follows: Correlations from H₂-7 (δ 2.04) to C-8 (δ 139.0) and from Me-26 (δ 42.5) and C-8 established the

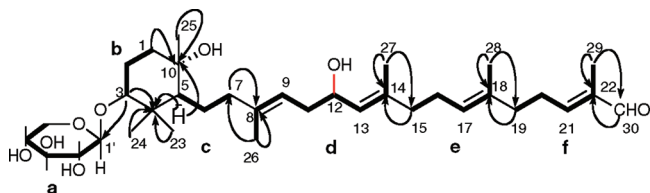


Figure 4. Selected ¹H–¹H COSY and HMBC correlations of **8**.

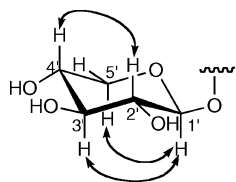


Figure 5. Selected NOESY correlations of **8**.

connectivity between **c** and **d**. The connectivity between **d** and **e** was deduced by the correlations from H₂-15 (δ 1.95–2.08) to C-14 (δ 138.0) and from Me-27 (δ 1.70) to C-14 and C-15 (δ 39.3). The connectivity between **e** and **f** was shown by the correlations from H₂-19 (δ 2.17) to C-18 (δ 133.7) and from Me-28 (δ 1.63) to C-18 and C-19 (δ 37.9). The aldehyde was located at C-22 (δ 139.4), on the basis of the correlations from aldehydic proton H-30 (δ 9.38) to C-22 and from Me-29 (δ 1.74) to C-22 and C-30 (δ 199.5). The location of the hydroxy group at C-12 was based on the low-field chemical shifts of H-12 (δ 4.38) and C-12 (δ 68.7), although the configuration was not determined. The geometries of the Δ^8 , Δ^{13} , Δ^{17} , and Δ^{21} double bonds were confirmed to be *E* on the basis of the chemical shifts of C-26 (δ 16.4), C-27 (δ 16.7), C-28 (δ 15.9), and C-29 (δ 9.2).¹³ The α -orientation of H-3, H-5, and Me-23 and the β -orientation of Me-24 and Me-25 were elucidated by the interpretation of the NOESY correlations from H-3 to H-5 and H-23 and from Me-24 to Me-25, respectively. Thus the relative configuration of rhabdastroside A is as shown in **8**. Rhabdastroside A is an extremely rare example of a monocyclic triterpene¹⁴ and is the first example to be isolated from a sponge.

The cytotoxicity of rhabdastins A–E (**1**–**5**) and G (**7**) and the diacetate (**11**) in human promyelocytic leukemia cells (HL-60) was determined by MTT assay. Compound **6** was not assayed because of its insufficient amount. Compounds **4**, **5**, **7**, and **11**, possessing a dioxycyclopentane side chain, exhibited weak activity with the following IC₅₀ values, **4** (21 μ M), **5** (29 μ M), **7** (44 μ M), and **11** (11 μ M), while compounds **1**, **2**, and **3**, with a 2-methyl propanoate side chain, were inactive at 100 μ M.

To elucidate the mechanism of the cytotoxicity of **4** and **5**, we measured the proportion of apoptotic cells by FACS analysis. The early stage of apoptosis is characterized by plasma membrane alterations, which can be detected by Annexin-V fluorescein staining.¹⁵ We thus examined the apoptotic HL-60 cells by staining with Annexin V-FITC. Flow cytometric analysis demonstrated that the proportion of apoptotic HL-60 cells that were positive for Annexin-V after incubation with compounds **4** (10 μ M) and **5** (10 μ M) for 72 h were 18% and 17%, respectively, and approximately 2-fold higher than that of control cells (Figure S1).

Apoptosis results from activation of members of the caspase family of aspartate-specific proteases.¹⁶ Since compounds **4** and **5** induced apoptosis, we investigated the levels of caspase 3 in HL-60 cells. The cells treated with compounds **4** and **5** at 10 μ M caused caspase 3 cleavage in HL-60 cells (Figure S2). Bcl-2 family members play a vital role in regulating the mitochondrial apoptotic pathway and regulate the activation of caspases.¹⁷ The expression of Bcl-2 is thought to be an antiapoptotic factor.¹⁷ Subsequent examination revealed that compounds **4** and **5** did not affect expression of Bcl-2 in HL-60 cells. These findings suggested that induction of apoptosis of HL-60 cells by **4** and **5** was dependent upon caspase 3 activation, and the expression of Bcl-2 is not involved in compounds **4** and **5**-induced apoptosis.

Experimental Section

General Experimental Procedures. Optical rotations were measured at 25 °C on a JASCO DIP-370S polarimeter. UV spectra were measured by using a Hitachi U-2001 double-beam spectrophotometer. IR spectra were recorded on a MASCO FT/IR 5300. NMR spectra were recorded with a Bruker AVANCE 600 NMR instrument using CDCl₃ as a solvent. Chemical shifts are given on a δ (ppm) scale (¹H, 7.26 ppm; ¹³C, 77.0 ppm as the internal standard). MS spectra were obtained with a JEOL JMS XD-303 instrument in the positive-ion mode. VCC separation was performed with silica gel 60H (Merck, 90% < 45 μ m). Column chromatography was carried out on silica gel 60 (Merck, 70–230 μ m). Silica gel 60F plates (Merck, 0.25 mm thick) were used for TLC. HPLC was performed using a Waters 501 HPLC pump with a Shodex UV-41 detector. A C₁₈ column (19 \times 150 mm) was used for HPLC.

Sponge Material. The sponge *Rhabdastrella globostellata* (collection number 263) was collected in the area of Amami-oshima Island (28°26'10" N, 129°36'23" E), Kagoshima Prefecture, Japan, on April 20, 2000, and was frozen immediately after collection. A voucher specimen has been deposited at the Faculty of Science, Kagoshima University (voucher specimen: 263-Rg), and also in the Zoological Museum of Amsterdam (ZMA Por. 16401).

Extraction and Isolation. The organism (wet weight 7.7 kg, dry weight 1.2 kg) was chopped into small pieces and extracted with MeOH three times. The dried MeOH extract was suspended in H₂O and extracted with CH₂Cl₂. The aqueous solution was further extracted with *n*-BuOH. A portion (7.1 g) of the CH₂Cl₂ extract (28.1 g) was subjected to column chromatography on silica gel. Fractions of 200 mL were collected as follows: 1 and 2 (CH₂Cl₂/*n*-hexane, 4:1), 3 and 4 (CH₂Cl₂), 5 and 6 (MeOH/CH₂Cl₂, 1:49), 7–9 (MeOH/CH₂Cl₂, 1:19), 10 and 11 (MeOH/CH₂Cl₂, 1:9), 12 and 13 (MeOH/CH₂Cl₂, 1:4), 14–17 (MeOH). Fractions 8 and 9 (3.8 g) were chromatographed on silica gel with MeOH/CH₂Cl₂ (1:49) and gave a fraction (3.3 g), which was esterified with trimethylsilyldiazomethane to yield 3.3 g of esterified material. This material was repeatedly subjected to silica gel column chromatography with MeOH/CH₂Cl₂ (1:49 to 1:19). Final purification was performed by reversed-phase HPLC with CH₃CN/H₂O (3:2 to 4:1) to yield compounds **1** (3.1 mg), **2** (0.7 mg), **3** (3.2 mg), **4** (3.7 mg), **5** (3.5 mg), **6** (1.7 mg), and **7** (1.6 mg). Further elution of the combined fraction 8/9 (3.8 g) with MeOH/CH₂Cl₂ (1:9) and treatment of the eluate with trimethylsilyldiazomethane, which was then further separated by silica gel chromatography (MeOH/CH₂Cl₂) followed by HPLC (CH₃CN/H₂O, 43/57), yielded compound **8** (0.7 mg).

Rhabdastin A (1): amorphous powder; [α]_D²⁵ –47.6 (*c* 0.14, MeOH); TLC *R*_f 0.72 (1:19 MeOH/CH₂Cl₂); UV (MeOH) λ _{max} (log ϵ) 245 (3.71) nm; IR (NaCl) ν _{max} 1738, 1723, 1640 cm⁻¹; ¹H NMR, see Table 2; ¹³C NMR, see Table 1; HRFABMS *m/z* 391.2480 [M + H]⁺ (calcd for C₂₃H₃₅O₅, 391.2493).

Rhabdastin B (2): amorphous powder; [α]_D²⁵ –62 (*c* 0.03, MeOH); TLC *R*_f 0.54 (1:49 MeOH/CH₂Cl₂); UV (MeOH) λ _{max} (log ϵ) 245 (3.80) nm; IR (NaCl) ν _{max} 1722, 1637 cm⁻¹; ¹H NMR, see Table 2; ¹³C NMR, see Table 1; HRFABMS *m/z* 349.2380 [M + H]⁺ (calcd for C₂₁H₃₅O₄, 349.2376).

Rhabdastin C (3): amorphous powder; [α]_D²⁵ –49.8 (*c* 0.14, MeOH); TLC *R*_f 0.33 (3:97 MeOH/CH₂Cl₂); UV (MeOH) λ _{max} (log ϵ) 245 (3.71) nm; IR (NaCl) ν _{max} 1738, 1639 cm⁻¹; ¹H NMR, see Table 2; ¹³C NMR, see Table 1; HRFABMS *m/z* 435.2394 [M + H]⁺ (calcd for C₂₄H₃₅O₇, 435.2367).

Rhabdastin D (4): amorphous, pale yellow powder; [α]_D²⁵ –23 (*c* 0.09, MeOH); TLC *R*_f 0.46 (1:19 MeOH/CH₂Cl₂); UV (MeOH) λ _{max} (log ϵ) 304 (4.22) nm; IR (NaCl) ν _{max} 3430, 1732, 1694, 1622 cm⁻¹; ¹H NMR, see Table 2; ¹³C NMR, see Table 1; HRFABMS *m/z* 513.3582 [M + H]⁺ (calcd for C₃₂H₄₉O₅, 513.3580).

Rhabdastin E (5): amorphous, pale yellow powder; [α]_D²⁵ –85.9 (*c* 0.14, MeOH); TLC *R*_f 0.47 (7:93 MeOH/CH₂Cl₂); UV (MeOH) λ _{max} (log ϵ) 304 (4.23) nm; IR (NaCl) ν _{max} 3410, 1732, 1692, 1622 cm⁻¹; ¹H NMR, see Table 2; ¹³C NMR, see Table 1; HRFABMS *m/z* 513.3574 [M + H]⁺ (calcd for C₃₂H₄₉O₅, 513.3580).

Rhabdastin F (6): amorphous, pale yellow powder; [α]_D²⁵ –160 (*c* 0.09, MeOH); TLC *R*_f 0.44 (7:93 MeOH/CH₂Cl₂); UV (MeOH) λ _{max} (log ϵ) 304 (4.38) nm; IR (NaCl) ν _{max} 3412, 1730, 1696, 1622 cm⁻¹; ¹³C NMR, ¹H NMR, see Table 2; see Table 1; HRFABMS *m/z* 513.3576 [M + H]⁺ (calcd for C₃₂H₄₉O₅, 513.3580).

Rhabdastin G (7): amorphous, pale yellow powder; [α]_D²⁵ –22.9 (*c* 0.13, MeOH); TLC *R*_f 0.49 (1:9 MeOH/CH₂Cl₂); UV (MeOH) λ _{max} (log ϵ) 304 (4.19) nm; IR (NaCl) ν _{max} 3391, 1734, 1694, 1620 cm⁻¹; ¹H NMR, see Table 2; ¹³C NMR, see Table 1; HRFABMS *m/z* 513.3683 [M + H]⁺ (calcd for C₃₂H₅₁O₆, 513.3686).

Rhabdastin H (8): amorphous powder; [α]_D²⁵ –180 (*c* 0.04, MeOH); TLC *R*_f 0.51 (1:9 MeOH/CH₂Cl₂); UV (MeOH) λ _{max} (log ϵ) 230 (4.11) nm; ν _{max} 3407, 1672, 1638 cm⁻¹; ¹H NMR (CDCl₃, 600 MHz) δ 9.38 (1H, s, H-30), 6.47 (1H, t, *J* = 7.1 Hz, H-21), 5.21 (1H, d, *J* = 8.5 Hz, H-13), 5.16 (1H, t, *J* = 6.7 Hz, H-9), 5.16 (1H, t, *J* = 6.7 Hz, H-17), 4.50 (1H, d, *J* = 5.4 Hz, H-1'), 4.38 (1H, ddd, *J* = 8.5, 8.5, 4.3 Hz, H-12), 4.07 (1H, dd, *J* = 12.0, 4.1 Hz, H-5'), 3.75 (1H, m, H-4'), 3.62 (1H, t, *J* = 7.1 Hz, H-3'), 3.50 (1H, dd, *J* = 12.0, 5.4 Hz, H-2'), 3.39 (1H, dd, *J* = 12.0, 7.6 Hz, H-5'), 3.25 (1H, dd, *J* = 11.6, 4.2 Hz, H-3), 2.45 (2H, dq, *J* = 14.7, 7.3 Hz, H-20), 2.31 (1H, overlapped, H-11), 2.17 (2H, t, *J* = 7.3 Hz, H-19), 2.09–2.15 (2H, m, H-16), 2.09 (1H, overlapped, H-11), 2.04–2.12 (2H, overlapped, H-7), 1.96 (1H, m, H-2), 1.95–2.08 (2H, m, H-15), 1.74 (3H, br s, H-29), 1.73 (1H, overlapped, H-1), 1.70 (3H, br s, H-27), 1.66 (3H, br s, H-26), 1.63 (3H, br s, H-28), 1.59 (1H, overlapped, H-6), 1.58 (1H, overlapped, H-2), 1.43 (1H, overlapped, H-6), 1.41 (1H, overlapped, H-1), 1.17 (1H, m, H-5), 1.13 (3H, s, H-25), 1.04 (3H, br s, H-23), 0.83 (3H, s, H-24); ¹³C NMR (CDCl₃, 150 MHz) δ 195.5 (C, C-30), 154.5 (CH, C-21), 139.4 (C, C-22), 139.0 (C, C-8), 138.0 (C, C-14), 133.7 (C, C-18), 127.7 (CH, C-13), 125.2 (CH, C-17), 121.0 (CH, C-9), 104.5 (CH, C-1'), 88.9 (CH, C-3), 73.9 (CH, C-3'), 72.6 (C, C-10), 72.3 (CH, C-2'), 69.7 (CH, C-47), 68.7 (CH, C-12), 63.8 (CH, C-5'), 54.2 (CH, C-5), 42.5 (CH₂, C-7), 40.7 (CH, C-1), 40.7 (C, C-4), 39.3 (CH₂, C-15), 37.9 (CH₂, C-19), 36.6 (CH₂, C-11), 28.2 (CH₃, C-23), 27.7 (CH₂, C-2), 27.4 (CH₂, C-20), 26.3 (CH₂, C-16), 23.3 (CH₂, C-6), 23.1 (CH₃, C-25), 16.7 (CH₃, C-27), 16.4 (CH₃, C-26), 15.9 (CH₃, C-24), 15.9 (CH₃, C-28), 15.9 (CH₃, C-29); HRFABMS *m/z* 605.4056 [M – H][–] (calcd for C₃₅H₅₇O₈, 605.4054).

***p*-Bromobenzoyl Ester of 4.** To a solution of compound **4** (9.8 mg) in CH₂Cl₂ (250 mL) were added *p*-bromobenzoyl chloride (10.2 mg), triethylamine (10 μ L), and DMAP (catalytic amount), and the mixture was stirred overnight at room temperature before concentration to give a crude mixture. The desired product was purified by silica gel chromatography and elution with mixtures of MeOH/CH₂Cl₂ followed by recrystallization from MeOH to yield the *p*-bromobenzoyl ester **10** (6.4 mg).

Rhabdastin D *p*-Bromobenzoate (10): colorless orthorhombic (MeOH), mp 202–203 °C; [α]_D²⁵ +25 (*c* 0.06, MeOH); TLC *R*_f 0.47 (7:93 MeOH/CH₂Cl₂); TLC *R*_f 0.66 (1:49 MeOH/CH₂Cl₂); UV (MeOH) λ _{max} (log ϵ) 304 (4.36) nm, 248 nm (4.23); IR (KBr) ν _{max} 3449, 1719, 1638, 1593, 1570 cm⁻¹; ¹H and ¹³C NMR, see Supporting Information; HRFABMS *m/z* 697.2921 [M + H]⁺ (calcd for C₃₉H₅₂O₆Br, 697.2921).

X-ray Analysis of 10. ¹⁸ Crystal data: C₃₉H₅₁BrO₆, colorless, orthorhombic, space group *P*2₁2₁2₁(#18), *a* = 16.6959(3) Å, *b* = 22.8458(4) Å, *c* = 9.30051(10) Å, *V* = 3547.51(10) Å³, *Z* = 4, *D*_{calc} 1.303 g/cm³, *F*₀₀₀ = 1472, μ (Cu K α) = 19.374 cm⁻¹. Intensity data were collected on a Rigaku RAXIS-RAPID diffractometer using monochromated Cu K α radiation (λ = 1.54187 Å) up to 2θ = 136.5°. Of the total 42 004, 6491 unique reflections were observed (*R*_{int} = 0.030). The structure was solved by direct methods (SIR97) and expanded using Fourier techniques (DIRDIF99). The non-hydrogen atoms were refined anisotropically. Hydrogen atoms were refined using their riding model. The Flack parameter was –0.023(9), which confirmed the absolute configuration. The final cycle of full-matrix least-squares refinement on *F*² was based on 6491 observed reflections and

424 variable parameters and converged with $R_1 = 0.0268$ (for 6100 reflections with $I > 2\sigma(I)$) and $wR_2 = 0.0601$ (for all the reflections). Atomic coordinates, bond lengths and angles, and thermal parameters have been deposited at Rigaku Corporation.

Acetylation of 5. Compound **5** (2.7 mg) was peracetylated with pyridine (10 drops), Ac_2O (10 drops), and DMAP (catalytic amount) to afford the triacetate **11** (1.1 mg).

Rhabdastin D Diacetate (11): amorphous powder; $[\alpha]_{\text{D}}^{25} -86$ (c 0.06, MeOH); TLC R_f 0.46 (1:49 MeOH/ CH_2Cl_2); UV (MeOH) λ_{max} ($\log \epsilon$) 300 (4.25) nm; IR (NaCl) ν_{max} 1736, 1696, 1624 cm^{-1} ; ^1H and ^{13}C NMR, see Supporting Information; HRFABMS m/z 597.3792 [$\text{M} + \text{H}]^+$ (calcd for $\text{C}_{36}\text{H}_{53}\text{O}_7$, 597.3792).

Cell Lines. Human leukemia HL-60 cells were maintained in RPMI1640 containing 10% fetal calf serum, 2 mM glutamine, and the antibiotic/antimycotic solution at 37 °C in a 5% CO_2 humidified atmosphere.

Annexin V Staining. Detection of plasma membrane alterations in HL-60 cells was performed using the Annexin V-FITC apoptosis detection kit (BioVision). Cells were treated with 10 μM compound **4** or **5** for 72 h, then washed once with PBS. For flow cytometry, cells (5×10^5) were suspended in 500 μL of binding buffer, and then 5 μL of Annexin-FITC was added. The mixtures were incubated at room temperature for 5 min in the dark. The levels of fluorescent staining of the cells were analyzed using a Beckman EPICS flow cytometer (Coulter Electronics).

Immunoblotting Analysis. Samples were subjected to 12.5% sodium dodecyl sulfate polyacrylamide gel electrophoresis (SDS-PAGE) according to the method of Laemmli.¹⁹ Gel proteins were electrophoretically transferred onto polyvinylidene difluoride membranes (Immobilon-P transfer membrane; Millipore) using the Bio-Rad Transblot SD apparatus. The membrane was treated with the buffer (350 mM NaCl, 10 mM Tris-HCl [pH 8.0], 0.05% Tween-20) containing 3% skimmed milk for 1 h and incubated overnight at 4 °C with the indicated antibody (1:1000) in the buffer containing 3% skimmed milk. Following four washes with the buffer (10 min each), the membrane was incubated with a peroxidase-conjugated horse anti-rabbit IgG diluted 1:1000 in the buffer containing 3% skimmed milk for 1 h. The membrane was washed with buffer and developed using the enhanced chemiluminescence western blotting detection system (Amersham Pharmacia).

Acknowledgment. We are grateful to Dr. D. Muanza at the Biotics Research Corporation, Rosenberg, Texas, and Dr. J. L. C. Wright, Center for Marine Science, University of North Carolina at Wilmington, for valuable discussions and interest in this study. We also thank Mrs. K. Babazono and N. Nishitani for the preliminary experiments.

Supporting Information Available: ^1H NMR and ^{13}C NMR spectra for **1–8**, **10**, and **11**, NMR spectroscopic data for **10** and **11** (Table

S1), and key HMBC and NOE spectroscopic data for **1–8** (Table S2). This material is available free of charge via the Internet at <http://pubs.acs.org>.

References and Notes

- Sashidhara, K. V.; White, K. N.; Crews, P. *J. Nat. Prod.* **2009**, *72*, 588–603, and references therein.
- Blunt, J. W.; Copp, B. R.; Hu, W.-P.; Munro, M. H. G.; Northcote, P. T.; Prinsep, M. R. *Nat. Prod. Rep.* **2007**, *24*, 31–86, and previous articles in the series.
- Recent examples: (a) Guo, J.-F.; Zhou, J.-M.; Zhang, Y.; Deng, R.; Liu, J.-N.; Feng, G.-K.; Liu, Z.-C.; Xiao, D.-J.; Deng, S.-Z.; Zhu, X.-D. *Cell. Biol. Int.* **2008**, *32*, 48–54. (b) Lv, F.; Xu, M.; Deng, Z.; de Voogd, N. J.; van Soest, R. M. W.; Proksch, P.; Lin, W. *J. Nat. Prod.* **2008**, *71*, 1738–1741. (c) Aoki, S.; Sanagawa, M.; Watanabe, Y.; Setiawana, A.; Arai, M.; Kobayashi, M. *Bioorg. Med. Chem.* **2007**, *15*, 4818–4828. (d) Fouad, M.; Edrada, R. A.; Ebel, R.; Wray, V.; Müller, W. E. G.; Lin, W. L.; Lin, Proksch, P. *J. Nat. Prod.* **2006**, *69*, 211–218. (e) Lv, F.; Deng, Z.; Li, J.; Fu, H.; van Soest, R. W. M.; Proksch, P.; Lin, W. *J. Nat. Prod.* **2004**, *67*, 2033–2036.
- Clement, J. A.; Li, M.; Hecht, S. M.; Kingston, D. G. I. *J. Nat. Prod.* **2006**, *69*, 373–376.
- Iwagawa, T.; Nishitani, N.; Nakatani, M.; Doe, M.; Morimoto, Y.; Takemura, K. *J. Nat. Prod.* **2005**, *68*, 31–35.
- Iwagawa, T.; Babazono, K.; Nakatani, M.; Doe, M.; Morimoto, Y.; Takemura, K. *Heterocycles* **2005**, *65*, 607–617.
- Iwagawa, T.; Babazono, K.; Nakatani, M.; Doe, M.; Morimoto, Y.; Shiro, M.; Takemura, K. *Heterocycles* **2005**, *65*, 2083–2093.
- Iwagawa, T.; Hashimoto, K.; Okamura, H.; Kurawaki, J.; Nakatani, M.; Hou, D.-X.; Fujii, M.; Doe, M.; Morimoto, Y.; Takemura, K. *J. Nat. Prod.* **2006**, *69*, 1130–1133.
- Iwagawa, T.; Miyazaki, M.; Yokogawa, Y.; Okamura, H.; Nakatani, M.; Doe, M.; Morimoto, Y.; Takemura, K. *Heterocycles* **2008**, *75*, 2023–2028.
- Tsuda, M.; Ishibashi, M.; Ageta, K.; Sasaki, T.; Kobayashi, J. *Tetrahedron* **1991**, *47*, 2181–2194.
- Flack, H. D. *Acta Crystallogr.* **1983**, *A39*, 876–881.
- Rudi, A.; Levi, S.; Benayahu, Y.; Kashman, Y. *J. Nat. Prod.* **2002**, *65*, 1672–1674.
- Couperus, P. A.; Clague, A. D. H.; van Dongen, J. P. C. M. *Org. Magn. Reson.* **1976**, *8*, 426–431.
- Barrero, A. F.; Alvarez-Manzaneda, R.; Alvarez-Manzaneda, R. *Tetrahedron Lett.* **1989**, *30*, 3351–3352.
- van Engeland, M.; Nieland, L. J.; Ramaekers, F. C.; Schutte, B.; Reutelingsperger, C. P. *Cytometry* **1998**, *31*, 1–9.
- Chowdhury, I.; Tharakan, B.; Bhat, G. K. *Comp. Biochem. Physiol. Part B: Biochem. Mol. Biol.* **2008**, *151*, 10–27.
- Yip, K. W.; Reed, J. C. *Oncogene* **2008**, *27*, 6398–6406.
- Crystallographic data for compound **10** have been deposited with the Cambridge Crystallographic Data Center (deposition number CCDC 754575).
- Laemmli, U. K. *Nature* **1970**, *227*, 680–685.

NP100302A